ORIGINAL ARTICLE

Cancer Science WILEY

FAXC interacts with ANXA2 and SRC in mitochondria and promotes tumorigenesis in cholangiocarcinoma

Haruna Fujimori[1] | Mao Shima-Nakamura[1] | Shin-Ichiro Kanno[2] |
Rie Shibuya-Takahashi[1] | Mai Mochizuki[1] | Masamichi Mizuma[3] | Michiaki Unno[3] |
Yuta Wakui[4] | Makoto Abue[4] | Wataru Iwai[4] | Daisuke Fukushi[5] | Kennich Satoh[5] |
Kazunori Yamaguchi[6] | Norihisa Shindo[7] | Jun Yasuda[6] | Keiichi Tamai[1]

[1]Division of Cancer Stem Cell, Miyagi Cancer Center Research Institute, Natori, Japan

[2]IDAC Fellow Research Group for DNA Repair and Dynamic Proteome Institute of Development, Aging and Cancer (IDAC), Tohoku University, Sendai, Japan

[3]Department of Surgery, Tohoku University Graduate School of Medicine, Sendai, Japan

[4]Department of Gastroenterology, Miyagi Cancer Center, Natori, Japan

[5]Division of Gastroenterology, Tohoku Medical and Pharmaceutical University, Sendai, Japan

[6]Division of Molecular and Cellular Oncology, Miyagi Cancer Center Research Institute, Natori, Japan

[7]Cancer Chromosome Biology Unit, Miyagi Cancer Center Research Institute, Natori, Japan

Correspondence
Haruna Fujimori, Division of Cancer Stem Cell, Miyagi Cancer Center Research Institute, 47-1 Medeshima-Shiote, Natori, Miyagi 981-1239, Japan.
Email: fuji.spr.na@gmail.com

Funding information
Kobayashi Foundation for Cancer Research; Japan Society for the Promotion of Science, Grant/Award Number: 19K08430, 20K09701, 21H02396, 21K07137, 21K07186, 21K07973, 22K07974, 22K08085, 22K09678 and 22K09696; Takeda Medical Research Foundation

Abstract

Cholangiocarcinoma (CCA) is one of the most difficult malignancies to treat as the therapeutic options are limited. Although several driver genes have been identified, most remain unknown. In this study, we identified a *failed axon connection homolog* (*FAXC*), whose function is unknown in mammals, by analyzing serially passaged CCA xenograft models. Knockdown of *FAXC* reduced subcutaneous tumorigenicity in mice. FAXC was bound to annexin A2 (ANXA2) and c-SRC, which are tumor-promoting genes. The FAXC/ANXA2/c-SRC complex forms in the mitochondria. FAXC enhances SRC-dependent ANXA2 phosphorylation at tyrosine-24, and the C-terminal amino acid residues (351–375) of FAXC are required for ANXA2 phosphorylation. Transcriptome data from a xenografted CCA cell line revealed that *FAXC* correlated with epithelial–mesenchymal transition, hypoxia, and KRAS signaling genes. Collectively, these findings advance our understanding of CCA tumorigenesis and provide candidate therapeutic targets.

KEYWORDS
ANXA2, cholangiocarcinoma, FAXC, SRC, tumorigenicity

1 | INTRODUCTION

Cholangiocarcinoma is the second most common liver malignancy after hepatocellular carcinoma. Over the past four decades, the overall incidence of CCA has progressively increased worldwide.[1] It is an aggressive tumor with limited treatment options besides surgery, and most patients present with advanced-stage disease.[2] Comprehensive genome/exome analyses have identified driver genes, such as *FGFR2*[3]; however, their clinical relevance remains unclear and novel therapeutic targets are needed.

One of the hallmarks of cancer is the maintenance of proliferative signaling, which results in tumorigenesis.[4] Xenograft mouse models can mimic the tumor microenvironment and reconstituted tumor tissues can resemble actual human tumor tissues.[5] Thus, xenograft mouse models serve as a gold standard for identifying highly tumorigenic cancer cells.[6] To develop new therapeutic strategies for CCA, we identified novel genes required for tumorigenesis using a xenograft model.

The proto-oncogene c-SRC is a tyrosine kinase involved in cancer development.[7] Annexin A2, a member of the annexin family, was originally identified as a substrate of v-SRC.[8,9] SRC is catalytically activated following Y416 autophosphorylation,[10] and Tyr24 phosphorylation of ANXA2 by SRC is an important posttranslational modification of ANXA2. This activates intracellular signaling pathways, such as the ERK and EMT pathways.[11,12] Annexin A2 is also required for tumorigenesis in breast cancer cells,[12] and its activity is regulated by phosphorylation.[13] Based on recent studies, c-SRC and ANXA2 coordinate to promote cancer development. In breast cancer, Rack1, which is a multifaceted scaffold protein, binds to SRC/ANXA2 and promotes invasion and metastasis.[14] The Ras-like proto-oncogene RalA forms a complex with SRC/ANXA2 and promotes ERK1/2 signaling in breast cancer[15]; however, the detailed molecular mechanisms of ANXA2 and SRC in cancer progression, particularly in CCA, are largely unknown. In this study, we identified a novel gene required for the progression and development of CCA using a xenograft mouse model.

2 | MATERIALS AND METHODS

2.1 | Ethics statements

This study was conducted according to the principles of the Declaration of Helsinki and was approved by the ethics committee of the Miyagi Cancer Center Research Institute. The animal experimental protocols were approved by the Miyagi Cancer Center Animal Care and Use Committee (permit number: AE.22.01).

2.2 | Tumor implantation

Xenograft passage was carried out as previously described.[5,16] Briefly, resected fresh tumor specimens were obtained from Tohoku University Hospital after obtaining written informed consent from the patients. The tumor tissues were minced with PBS on ice, washed three to six times with PBS, and incubated with collagenase/dispase and DNAse. After five washes with PBS, the cell pellet was suspended in lysis buffer and 2% FBS in PBS was added. The cell suspension was mixed with Matrigel and transplanted subcutaneously into NOG mice (In-Vivo Science). When the tumors grew to approximately 1 cm in diameter, the mice were killed. The tumor tissue was resected, minced, and transplanted into a new mouse using Matrigel.

2.3 | Cell lines

The methods are described in Appendix S1.

2.4 | Generation of lentiviral particles and shRNA knockdown

For long-term silencing, CHOL1 cells expressing *FAXC*-specific shRNA were established using the MISSION lentiviral-based shRNA vector collection (Merck). To produce lentiviral particles, 293T cells were cultured in DMEM supplemented with low glucose and 10% FBS. The cells were seeded into 6-well plates and cotransfected with pCMV-VSV-G-RSV-Rev, pCAG-HIVgp, and a lentiviral plasmid vector (MISSION pLKO.1-puro) encoding short hairpins that target FAXC mRNA (MISSION shRNA TRCN0000142017 and MISSION shRNA TRCN TRCN0000141386) using the calcium phosphate method. pLKO.1 puro containing scrambled shRNA was used as the control lentiviral plasmid vector. After 72 h, the supernatant containing the lentiviral particles was filtered through a 0.45 μm syringe filter and transduced into CCA cells. The target cells were seeded at a density of 6×10^5 cells/well in 6-well plates. Fresh lentiviral particles were added. After 3 days, the cells were transferred to a medium containing puromycin.

2.5 | Gene expression profiles

Microarray analysis (SurePrint G3 $8 \times 60k$; Agilent) was undertaken to establish an expression profile for siFAXC-treated CHOL1 cells as previously described.[17] Data processing was carried out using R statistical software (version 3.6.3[18]) and GSEA software (Broad Institute, https://www.gsea-msigdb.org/gsea/index.jsp). A time-series analysis was undertaken using maSigPro.[19]

RNA was isolated from CHOL1 xenografts and used for sequencing. RNA was extracted from the resected tumors using RNeasy based on the manufacturer's protocol. Libraries were prepared by Rhelixa using the NEBNext Poly(A) mRNA Magnetic Isolation Module and NEBNext Ultra II Directional RNA Library

Prep Kit (New England Biolabs), and sequenced on a NovaSeq 6000 (Illumina). Raw sequencing reads were aligned to human (hg38) and mouse (mm10) genomes using STAR,[20] and human-specific reads were selected using XenofilteR.[21] The data were annotated and counted using featurecount[22] and normalized with DESeq2.[23] Pathway enrichment analysis was carried out using GSEA.[24]

2.6 | In vivo tumorigenesis assay

A tumor formation assay was carried out as described previously.[16] Briefly, the cells were suspended in 50 μL PBS and an equal volume of Matrigel (BD Biosciences) on ice and injected into NOG mice with a 1 mL syringe. Tumor formation was monitored weekly and tumor volume was calculated using the following formula: 1/2 (length × width × height).

2.7 | In vitro cell assay

The specific methods are described in Appendix S1 and Table S1A,B.

2.8 | Construction of plasmid vector

The specific plasmid construction methods are described in Appendix S1 and Table S1C.

2.9 | Immunoprecipitation and nano-LC–MS/MS

Immunoprecipitation and nano-LC–MS/MS were carried out as described previously to identify the proteins associated with FAXC.[25–27] Cell lysates derived from CHOL1-PB-FAXC cells were immunoprecipitated with anti-FLAG M2 affinity gel #A2220 (Sigma-Aldrich), and the proteins were eluted using lysis buffer containing the FLAG peptide. The eluted proteins were separated by SDS-PAGE and detected using a silver staining kit for MS (Wako). The target bands were cut, decolorized, dehydrated, reduced, alkylated, and incubated with trypsin after washing. The resulting peptides were desalted using a Ziptip c18 (Millipore) and analyzed using a nano-LC–MS/MS system (DiNa HPLC system, KYA TECH Corporation/QSTAR XL, Applied Biosystems).

2.10 | Western blot analysis

The specific methods are described in Appendix S1 and Table S1D.

2.11 | Coimmunoprecipitation assay

The specific methods are described in Appendix S1.

2.12 | Purification of FAXC proteins and in vitro kinase assay

Purified ANXA2-His (#9409-AN-050) and c-SRC (#14-326-M) were purchased from Sigma-Aldrich and Funakoshi, respectively. Wild-type FAXC-His and delta 351–409-FAXC were purified from transformed Rosetta-gami B(DE3) competent cells (#71136-3CN; Sigma-Aldrich) as described previously.[28-30] Briefly, transformed *Escherichia coli* were grown in 200 mL LB medium to an OD_{600} of 0.6 and incubated with 1 mM isopropyl beta-D-1-thiogalactopyranoside overnight at 18°C. The *E. coli* culture was centrifuged and the resulting pellet was re-suspended in lysis buffer (200 mM NaCl, 10 mM imidazole, 1 mg/mL lysozyme, 20 mM Tris–HCl, pH 7.5) with cOmplete Mini Protease Inhibitor Cocktail (Roche) and lysed by ultrasonication. The lysates were centrifuged and the resulting pellet was resuspended in lysis buffer containing 6 M guanidine–HCl. His-tag purification was carried out using HisTrap (HP #17524701; Cytiva). Because His-FAXC is insoluble, dialysis and refolding were required. Therefore, stepwise dialysis with L-arginine was done as described previously.[31]

A kinase assay was carried out as described previously with minor modifications.[32] The purified proteins were incubated with kinase buffer (50 mM HEPES pH 7.8, 5 mM $MgCl_2$, 150 mM NaCl, 1 mM DTT, 10 mM ATP) plus PhosSTOP (Roche) for 1 h at 30°C.

2.13 | Immunofluorescent staining and mitochondrial isolation

The specific methods are described in Appendix S1 and Table S1D.

2.14 | In situ hybridization

A CCA tissue microarray (#GA802a) was purchased from TissueArray.com (Derwood). *FAXC* mRNA in the tissue microarray was detected using an RNAscope 2.5 HD Assay-BROWN (Advanced Cell Diagnostics) based on the manufacturer's instructions. The probes used were as follows: Hs-FAXC-C1 (#1217261-C1), Positive Control probe (Hs-PPIB #313901), and Negative Control Probe (dapB #310043).

2.15 | Immunohistochemistry

The specific methods are described in Appendix S1 and Table S1D.

2.16 | Statistical analysis

Statistical analysis was undertaken using GraphPad Prism Vision 10.0.2 software (GraphPad. Software). Differences between the two groups were analyzed using an unpaired *t*-test. $*p < 0.05$, $**p < 0.01$, $***p < 0.001$, and $****p < 0.0001$ were considered statistically significant. All data are expressed as the mean ± SEM and represent the results of three independent experiments.
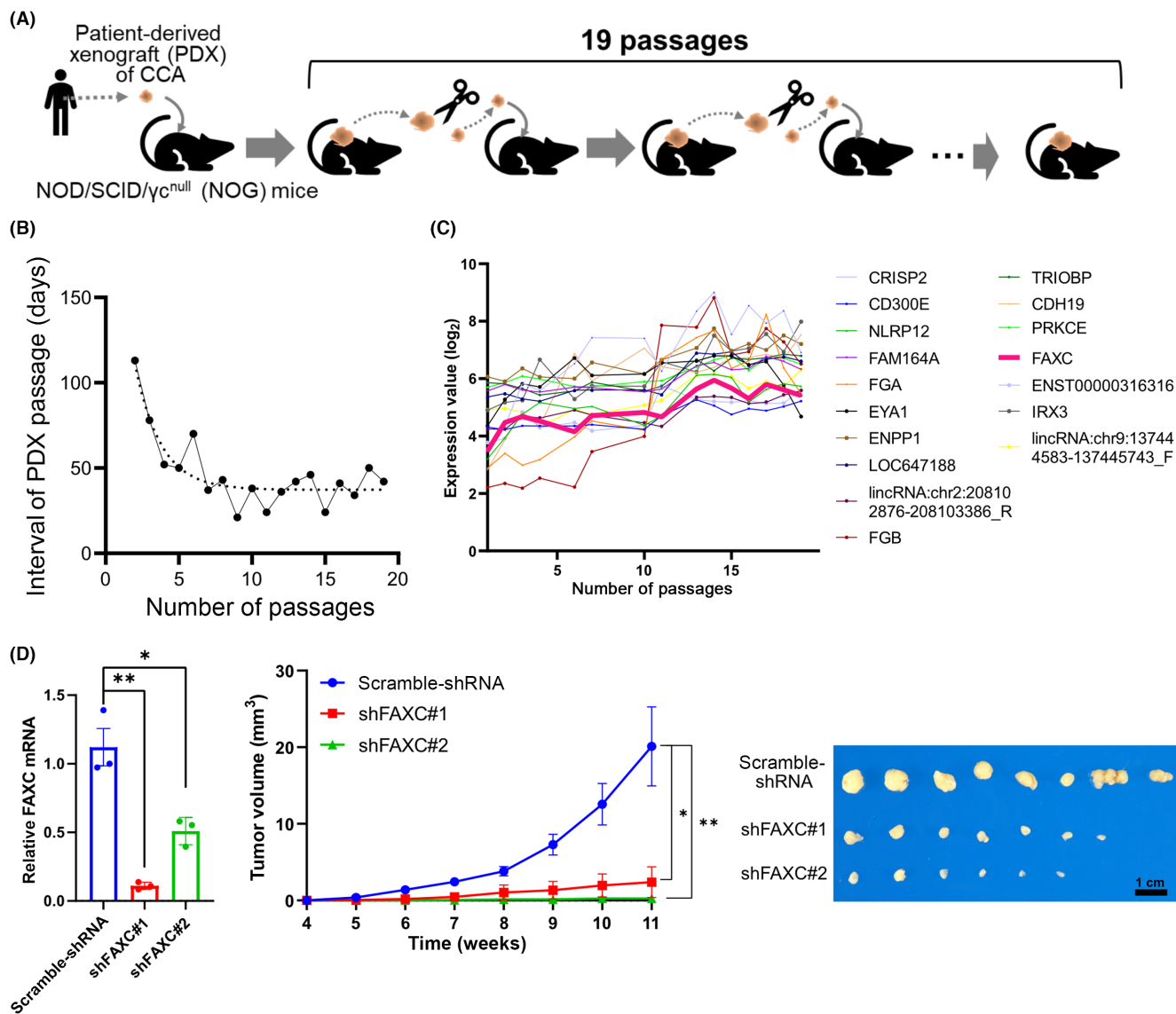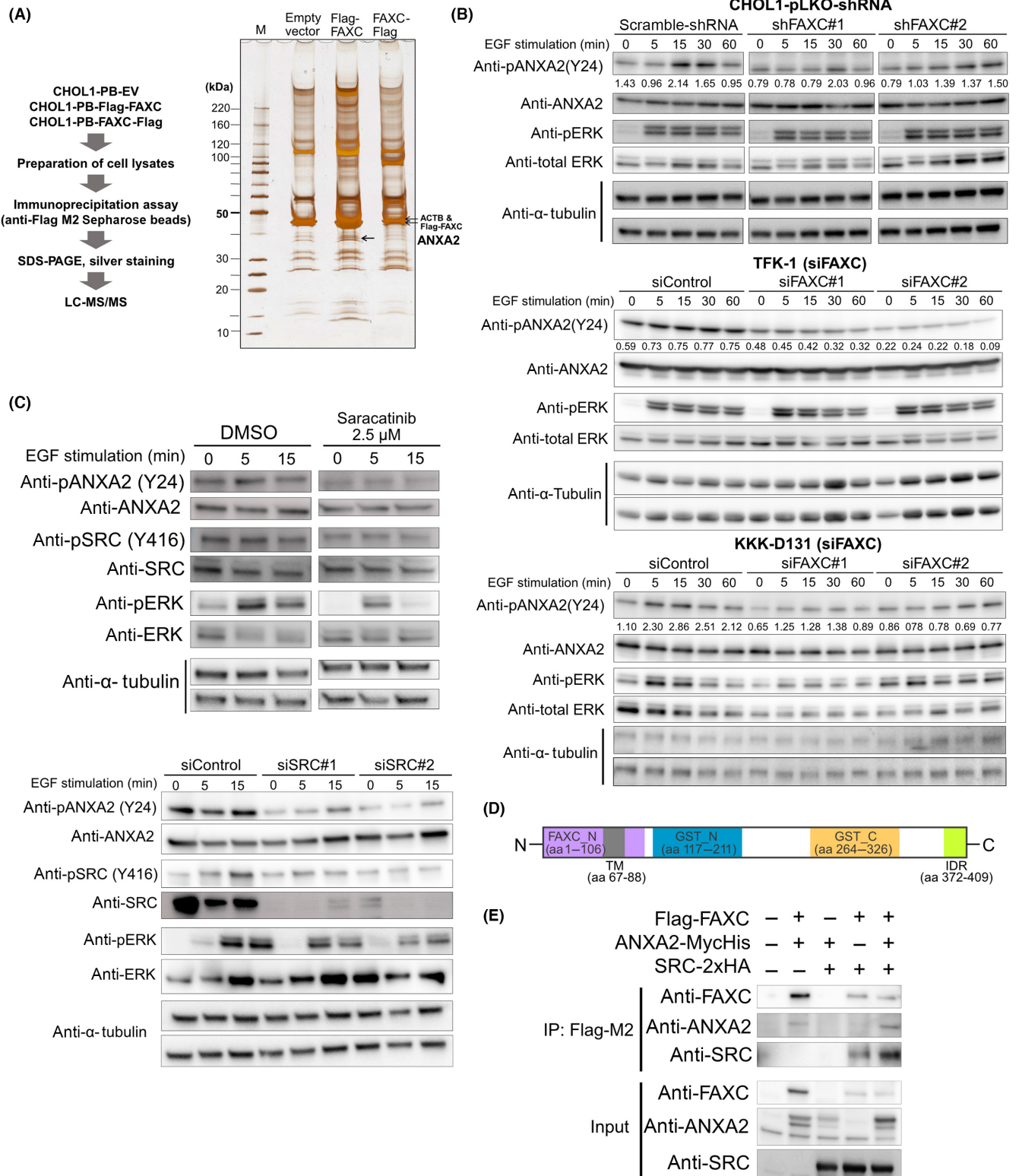
FIGURE 1 Identification of *Failed axon connection homolog* (*FAXC*) as an essential gene for tumor development in cholangiocarcinoma (CCA). (A) The experimental design for the identification of differentially expressed genes required for tumorigenesis. CCA patient-derived xenograft (PDX) was transplanted subcutaneously into mice and successively transferred to new mice. (B) Time intervals to passage. The tumors were passaged once they were approximately 1 cm in diameter. (C) Gene Cluster 6 based on a time series analysis. *FAXC* is shown as a bold line. (D) Tumorigenicity in NOG mice. Right panel, images of resected tumors from the control and *FAXC*-knockdown cells at 11 weeks following transplantation into mice. Center panel, quantitation of the tumor size for the control and *FAXC*-knockdown CHOL1 cells at the indicated time (*n*=8). Left panel, *FAXC* mRNA expression in CHOL1-pLKO-shFAXC cell lines (n=3). *$p < 0.05$, **$p < 0.01$.

FIGURE 2 Failed axon connection homolog (FAXC) interacts with annexin A2 (ANXA2) and c-SRC. (A) Left, experiment flowchart. Right, image of the silver-stained gel. Total cell lysates from CHOL1 cells stably expressing Flag-FAXC were coimmunoprecipitated with anti-FLAG Ab. Nine bands were identified relative to the empty vector cell lines and analyzed by liquid chromatography–tandem mass spectrometry. (B) Western blot analysis of *FAXC*-knockdown CHOL1, KKK-D131, and TFK-1. Following serum starvation, the cells were incubated with epidermal growth factor (EGF) and harvested at the indicated times. The values at the bottom of the anti-ANXA2 (Y24) panel indicate the level of ANXA2 phosphorylation and the values were calculated by dividing the band densities of the pANXA2 (Y24) by each total ANXA2. (C) Western blot analysis of SRC-inhibited CHOL1 cells. Following serum starvation for 24 h, CHOL1 cells were treated with saracatinib, an SRC inhibitor, for 3 h and stimulated with EGF. In SRC-knockdown CHOL1 cells, after siSRC transfection for 24 h, the cells were serum-starved for 24 h and stimulated with EGF. Cells were harvested at the indicated times. (D) Structure of the human FAXC protein. The domains were annotated using the HMMER and Conserved Domain Database. (E) Coimmunoprecipitation (IP) assay. *Flag-FAXC*, *ANXA2-Myc-His*, and *SRC-HA* expression vectors were transfected into 293T cells. After 2 days, the cells were harvested and total cell lysates were coimmunoprecipitated with anti-FLAG Ab. Aa, amino acid; FAXC_N, FAXC homolog N-terminus; GST_C, GST C-terminal domain; GST_N, GST N-terminal domain; IDR, intrinsically disordered region; TM, transmembrane region.

(A)

CHOL1-PB-EV
CHOL1-PB-Flag-FAXC
CHOL1-PB-FAXC-Flag

⬇

Preparation of cell lysates

⬇

Immunoprecipitation assay
(anti-Flag M2 Sepharose beads)

⬇

SDS-PAGE, silver staining

⬇

LC-MS/MS

(B)

(C)

(D)

(E)

3 | RESULTS

3.1 | FAXC is required for CCA tumorigenesis

Serially transplanted xenografts in immunodeficient mice are enriched in a subset of cells that show tumor reconstruction activity.[33] Therefore, we focused on genes showing an upward trend to identify novel genes essential for CCA development. Patient-derived human CCA cells (CHOL1) were subcutaneously implanted into NOG mice and serially passaged into new mice (Figure 1A). The PDX passage intervals were shorter with each generation (Figure 1B), suggesting that cells showing a high tumor reconstitution capacity were enriched through passaging. Tumor samples were collected at each passage and gene expression microarray analysis was carried

out. A time-series analysis revealed clusters with an upward trend, particularly Cluster 6 (Figures 1C and S1A). We selected candidate genes from Cluster 6 that were not previously reported to be associated with cancer. A second screening was carried out using a

tumorigenicity assay with siRNAs (data not shown). We found that *FAXC* altered tumorigenicity. The *FAXC* gene was upregulated through the passaging of cells (Figure 1C) and *FAXC* knockdown in CHOL1 cells resulted in the suppression of tumor development in
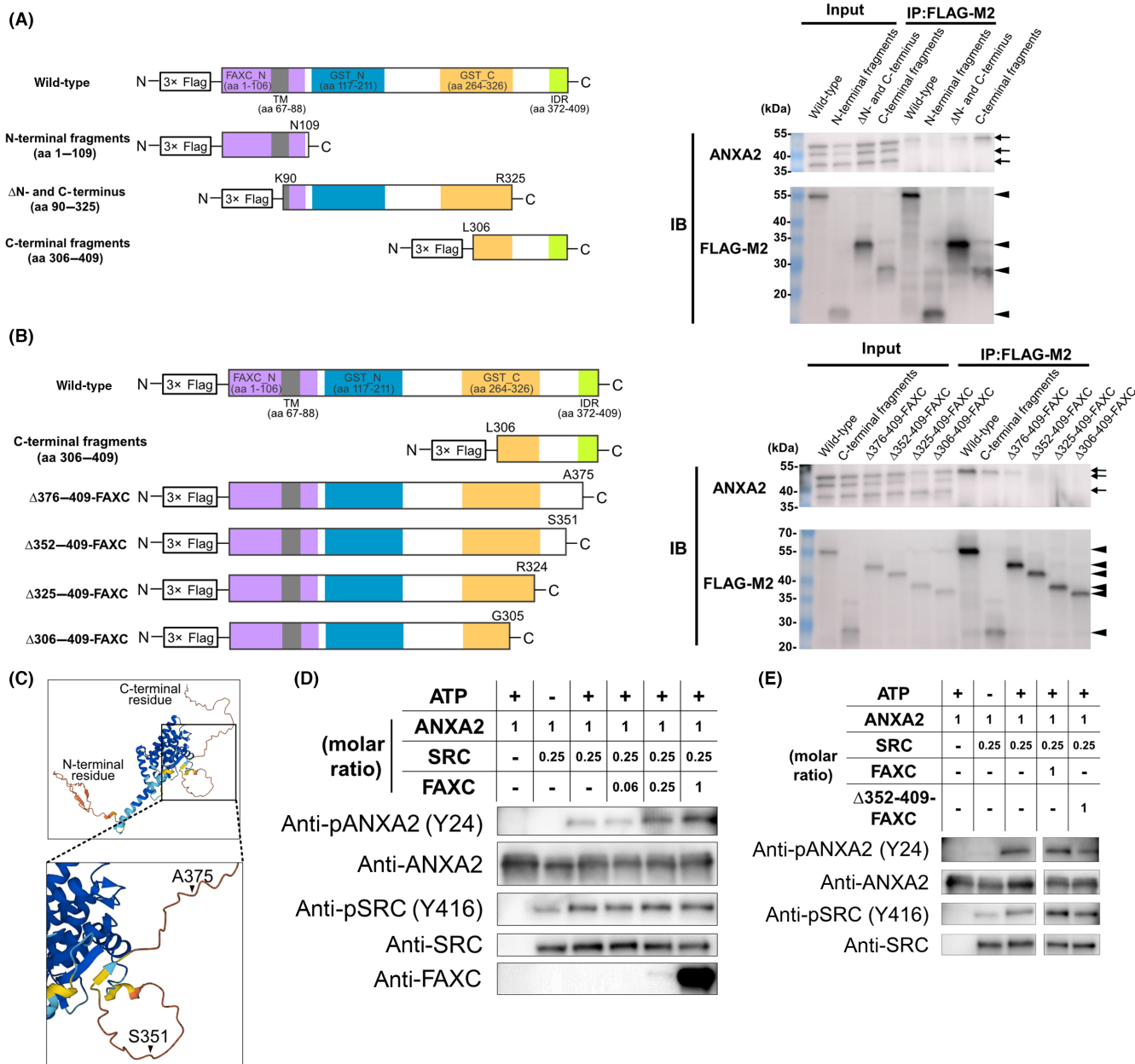
FIGURE 3 C-terminal region of failed axon connection homolog (FAXC) interacts with annexin A2 (ANXA2) for phosphorylation through SRC. (A) Left, schemas of the FAXC mutants. Right, coimmunoprecipitation (co-IP) assay of the FAXC mutants with ANXA2. *FAXC* mutants and WT *ANXA2-Myc-His* were transfected into 293T cells. Total cell lysates were coimmunoprecipitated with the anti-FLAG Ab. Arrows, ANXA2; arrowheads, FLAG-FAXC and its mutants. (B) Left, schemas of the ΔC-terminal FAXC mutants. Right, co-IP assay of the ΔC-terminal FAXC mutants with ANXA2 as described in (A). (C) Predicted 3D structure of the FAXC protein. The identified domain that binds to ANXA2 is shown in the inset. The prediction model was generated by AlphaFold. Colors indicate a per-residue confidence score (pLDDT). Blue, light-blue, yellow, and orange indicate very high (pLDDT >90), confident (90> pLDDT >70), low (70> pLDDT >50), and very low (pLDDT <50), respectively. (D) In vitro kinase assay. Recombinant ANXA2, SRC, and His-FAXC proteins were mixed and incubated in the presence of ATP. The reaction mixture was analyzed by western blotting. (E) In vitro kinase assay as described in (D). His-tag Ab and FAXC Ab had limited sensitivity and recombinant proteins were not able to determine the concentration in this experiment. Quantification of recombinant FAXC proteins was undertaken by measuring A260. aa, amino acid; Ab, antibodies; FAXC_N, FAXC homolog N-terminus; GST_C, GST C-terminal domain; GST_N, GST N-terminal domain; IB, immunoblot; IDR, intrinsically disordered region; TM, transmembrane region.

NOG mice (Figures 1D and S1B). These data suggest that *FAXC* is involved in tumorigenesis.

3.2 | FAXC interacts with ANXA2, a tumor-aggressive factor

FAXC homologous proteins are conserved between invertebrates and vertebrates (Figure S2); however, their molecular functions in mammalian cells have not been elucidated. To clarify the role of

FAXC, we identified a FAXC binding partner, ANXA2, by immunoprecipitation–MS analysis (Figures 2A and S3A). We then determined whether FAXC affected the phosphorylation of ANXA2 at Y24 in CCA cells. Phospho-ANXA2 levels were decreased and/or slowly induced following *FAXC* knockdown compared with control cells in three cell lines (Figures 2B and S3B). c-SRC is a tyrosine kinase involved in ANXA2 phosphorylation and our microarray data revealed that *FAXC* knockdown was correlated with the SRC-related pathway (Figure S3C). ANX A2 phosphorylation was also attenuated by treatment with SRC inhibitor and siSRC,
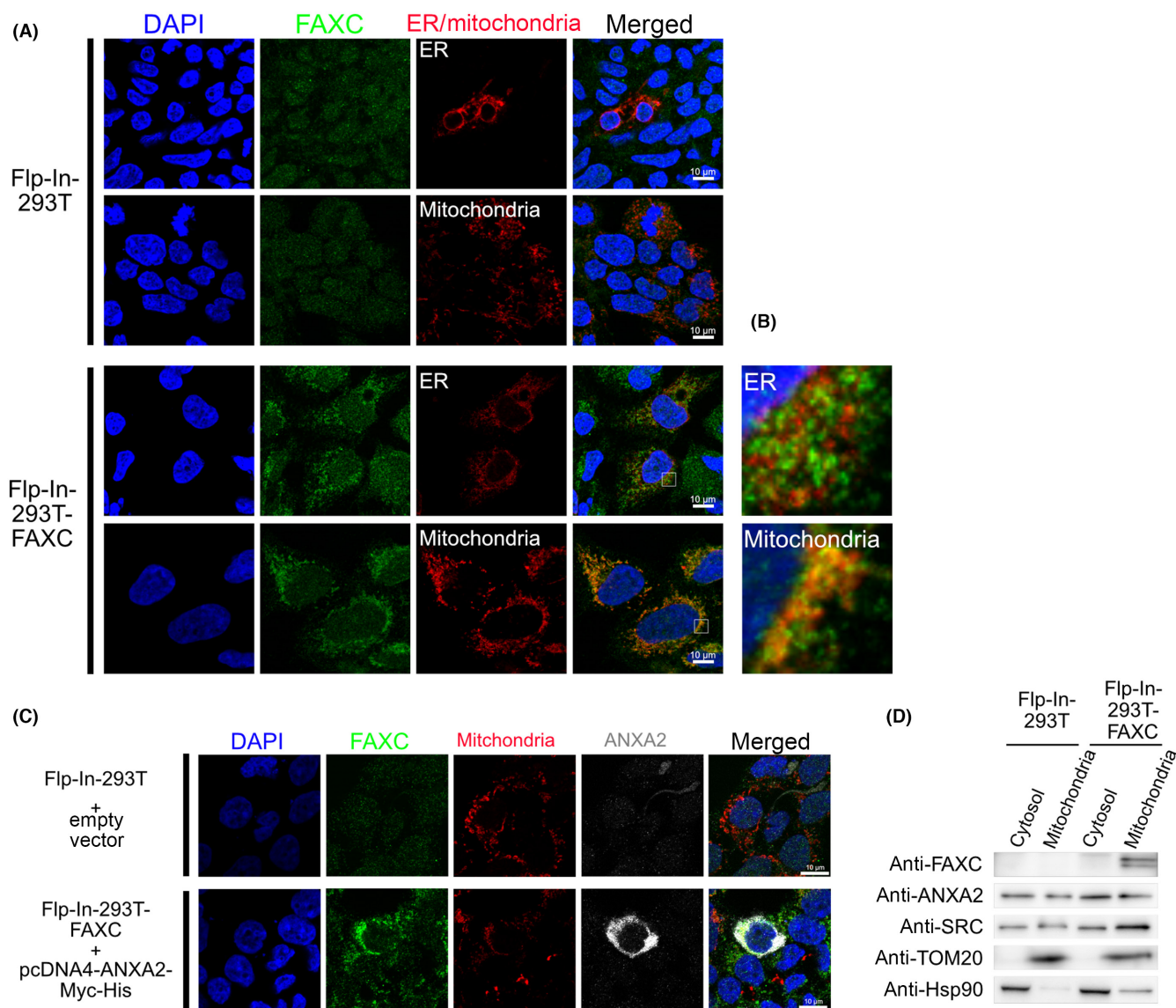

FIGURE 4 Failed axon connection homolog (FAXC), annexin A2 (ANXA2), and c-SRC localization at the mitochondria. (A) Subcellular localization of FAXC. Flp-In-293T-FAXC cells were coimmunostained to detect FAXC, endoplasmic reticulum (ER), and the mitochondria. The FAXC expression was induced by doxycycline (DOX) in Flp-In-293T-FAXC cells. (B) Higher magnification of the areas boxed in the image of Flp-In-293T-FAXC are shown in (A). (C) Immunofluorescent assay for FAXC and ANXA2. Flp-In-293T-FAXC cells were transfected with pcDNA4-ANXA2-Myc-His and incubated with DOX to induce FAXC. Blue, nucleus; green, FAXC; red, MitoTracker; gray, ANXA2. (D) Western blot analysis. Flp-In-293T-FAXC cells were incubated with DOX and lysed. Total cell lysates were fractionated into mitochondrial and cytosolic fractions and subject to western blot analysis. Anti-TOM20 and anti-Hsp60 Abs were used as the mitochondria- and cytosol-specific markers, respectively. Samples were loaded at equivalent protein weights. Parental Flp-In-293T cells were used as negative controls in all experiments.

concomitantly with the attenuation of c-SRC phosphorylation at Y416 in CHOL1 cells (Figure 2C), suggesting that ANXA2 phosphorylation is dependent on c-SRC activity. Based on a database of protein domains, FAXC does not have a kinase domain (Figure 2D). Thus, we hypothesized that the FAXC protein acts as a scaffold or an adapter protein[34] to bring the two proteins together and induce a relatively stable complex of ANXA2 and c-SRC. Therefore, we determined whether FAXC, ANXA2, and c-SRC form a protein complex. *Flag-FAXC*, *ANXA2-Myc-His*, and *SRC-2×HA* were transfected into 293T cells and a coimmunoprecipitation assay was carried out. As shown in Figure 2E, flag-FAXC was bound to both ANXA2 and SRC.

To determine the binding domain of FAXC that interacts with ANXA2, we designed FLAG-tagged FAXC deletion mutants (Figure 3A). Each FLAG-tagged deletion mutant and ANXA2-Myc-His were transiently coexpressed in 293T cells, and a coimmunoprecipitation assay was carried out. ANXA2 was found to immunoprecipitate with only the C-terminal fragments of FAXC (Figures 3A and S3D). We designed FAXC mutants with deletions in the C-terminal region (Figure 3B). ANXA2 coimmunoprecipitated with the WT and Δ376–409-FAXC proteins, but not with the other mutants (Figure 3B). These results suggest that the C-terminal region, residues 351–375, of FAXC are required for its interaction with ANXA2 (Figures 3C and S2). Taken together, these data indicate that FAXC acts as a scaffold for SRC and ANXA2 and promotes ANXA2 phosphorylation.

3.3 | FAXC enhances phosphorylation at Y24 by SRC

To confirm whether FAXC enhances the phosphorylation of ANXA2 at Y24 through SRC, in vitro kinase assays were carried out. ANXA2 was phosphorylated by c-SRC in the presence of ATP and this phosphorylation was enhanced by FAXC in a dose-dependent manner (Figure 3D). As reported above, the C-terminal region, residues 351–375, are required for the FAXC/SRC/ANXA2 complex to form. Thus, we prepared His-Δ376–409-FAXC, which lacks the C-terminal region, including 351–375 (Figure S4). The

phosphorylation levels of ANXA2 at Y24 were decreased in the presence of Δ376–409-FAXC proteins compared with the WT FAXC proteins (Figure 3E).

3.4 | FAXC localizes to mitochondria

Immunocytochemistry was undertaken for FAXC and the organelle markers. As shown in Figure 4A, FAXC primarily colocalized with the mitochondria compared with the endoplasmic reticulum (Figures S5 and 4A,B). FAXC was also colocalized with ANXA2 and the mitochondria (Figure 4C). We confirmed the intracellular localization of FAXC by cell fractionation. FAXC was primarily detected in the mitochondrial fraction, and ANXA2 and SRC were also present in this fraction (Figure 4D). These data suggest that FAXC might function in the mitochondria.

3.5 | FAXC expressed in human CCA and involves hypoxia, EMT, and the KRAS pathway in CCA tumors

We examined the distribution of FAXC in human CCA specimens. Because no suitable anti-FAXC Ab is available for immunohistochemistry, in situ hybridization was carried out by staining *FAXC* mRNA in formalin-fixed, paraffin-embedded human CCA specimens. *FAXC* mRNAs were observed in CCA tumor cells (Figure 5A) and *FAXC* mRNA-positive cells were present in small populations of the CCA tumor tissues. Furthermore, we analyzed The Cancer Genome Atlas dataset and found that *FAXC* mRNA expression was significantly higher in tumors compared with that in adjacent normal tissues (Figure 5B).

Finally, we determined how FAXC regulates CCA progression. To identify altered intracellular signaling pathways, *FAXC* knockdown CHOL1 cells were subcutaneously transplanted into NOG mice. The resulting tumor tissues were subjected to RNA sequencing analysis (Figure 5C,D). As shown in the figure, *FAXC* downregulation was negatively correlated with hypoxia and EMT gene sets in the hallmark gene sets (Table 1). Among the oncogenic genes, *KRAS*-related gene sets (KRAS.LUNG_UP.V1_UP and KRAS.LUNG.BREAST_UP.V1_UP) were strongly suppressed in

FIGURE 5 The Failed axon connection homolog (FAXC) is expressed in human cholangiocarcinoma and regulates hypoxia and epithelial–mesenchymal transition-related pathways. (A) Representative images of *FAXC* expression in cholangiocarcinoma tissues using the RNAscope assay. Black arrows indicate representative *FAXC*-positive spots. The probes used were as follows: Hs-FAXC-C1 (#1217261-C1), positive control probe (Hs-PPIB #313901), and negative control Probe (dapB #310043). Bar: low-magnification images, 20 μm; high-magnification images, 10 μm. (B) *FAXC* mRNA expression levels in The Cancer Genome Atlas (TCGA) Cholangiocarcinoma dataset. A total of 44 cases were analyzed and the values were calculated as fragments per kilobase of transcript per million (FPKM). (C) Experimental design for acquiring transcript profiles. (D) Expression levels of *FAXC* mRNA in transplanted CHOL1-pLKO-shFAXC cell lines for RNA sequencing. Real-time PCR was carried out. (E) Western blot analysis of hypoxia-inducible factor 1-α (HIF1-α) in CHOL1-pLKO-shFAXC cells. Normoxia was designated as 5% CO_2 at 37°C and hypoxia was considered 1% O_2, 5% CO_2, and 94% N_2 at 37°C for 62 h. (F) Representative images of immunohistochemical staining of HIF1-α in transplanted CHOL1-pLKO-shFAXC cells. Brown staining in the nucleus indicates HIF1-α-positive cells. Bar, 20 μm. (G) Western blot analysis of phosphorylated ANXA2 and STAT3 levels in CHOL1-pLKO-shFAXC cell lines. Cells were stimulated with epidermal growth factor (EGF) after serum starvation. Values at the bottom of the anti-pSTAT3 (Y705) or anti-pSTAT3 (Y727) panel indicate STAT3 phosphorylation levels and the values were calculated by dividing the band densities of the pSTAT3 by each total STAT3. **$p < 0.01$, ***$p < 0.001$.
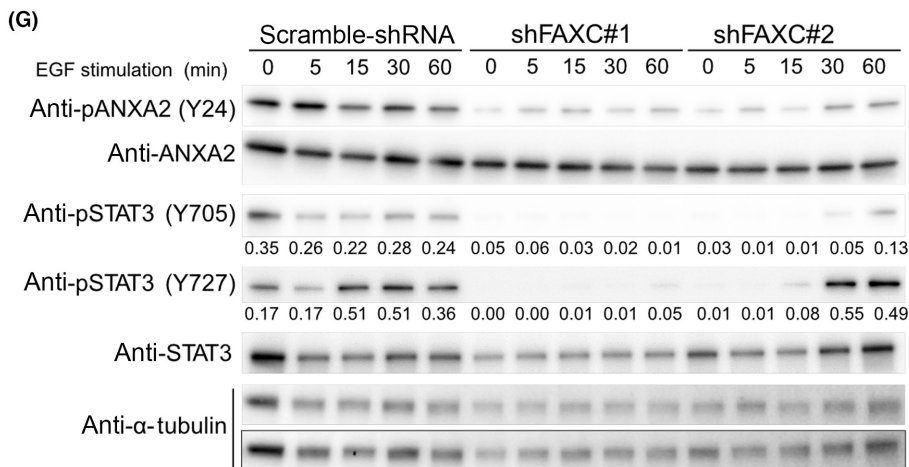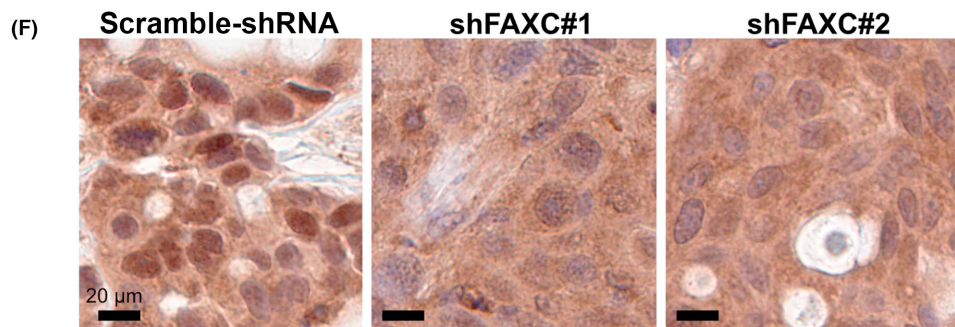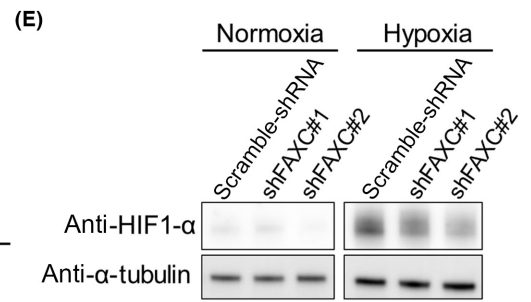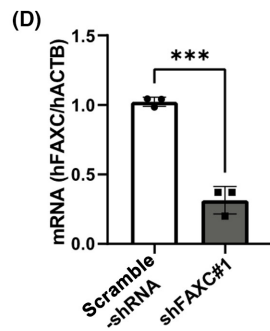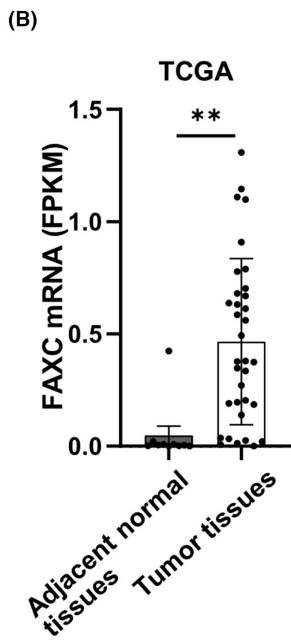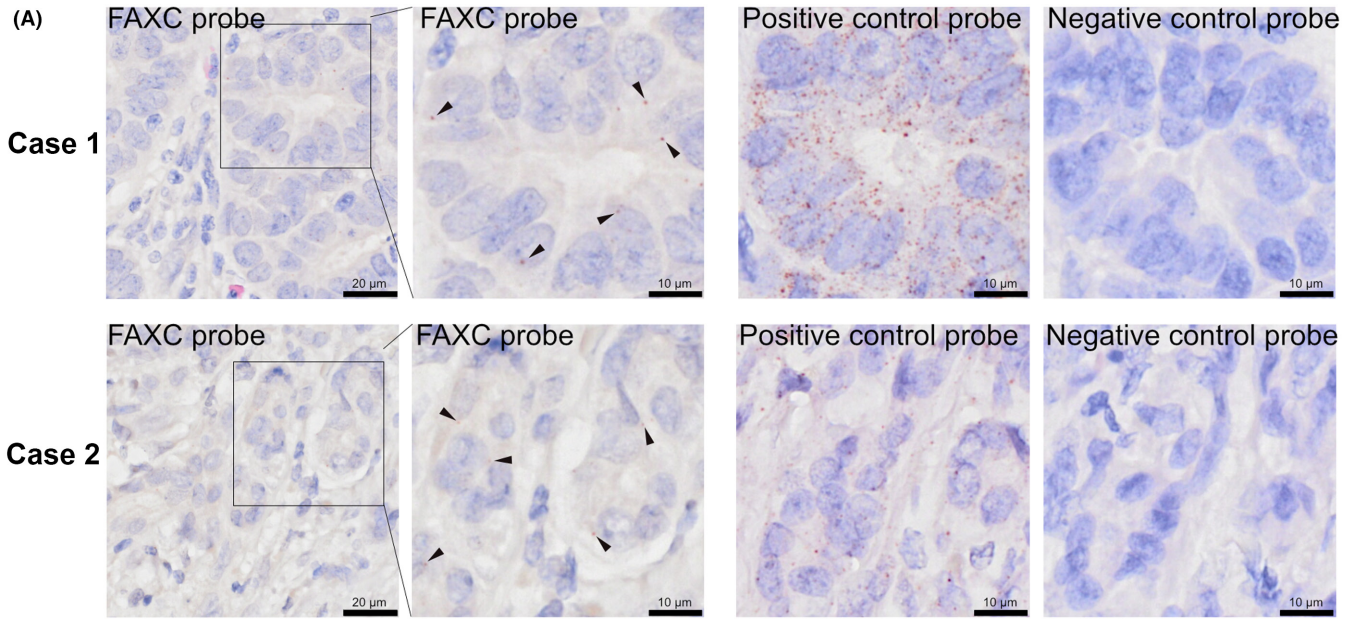
TABLE 1 Enrichment results of H: HALLMARK analyzed by Gene Set Enrichment Analysis.

Gene set	Enrichment score	p value	FDR q value
HALLMARK_HYPOXIA	0.5217	0.000	0.00000
HALLMARK_EPITHELIAL_MESENCHYMAL_ TRANSITION	0.4987	0.000	0.00000
HALLMARK_COMPLEMENT	0.4712	0.000	0.00000
HALLMARK_TNFA_SIGNALING_VIA_NFKB	0.4658	0.000	0.00000
HALLMARK_COAGULATION	0.4914	0.000	0.00000
HALLMARK_KRAS_SIGNALING_UP	0.4387	0.000	3.60E-04
HALLMARK_IL2_STAT5_SIGNALING	0.4328	0.000	4.73E-04
HALLMARK_IL6_JAK_STAT3_SIGNALING	0.4880	0.000	9.88E-04
HALLMARK_ANGIOGENESIS	0.5635	0.005	0.00157
HALLMARK_INFLAMMATORY_RESPONSE	0.4070	0.000	0.00202
HALLMARK_HEDGEHOG_SIGNALING	0.5196	0.011	0.00418
HALLMARK_ALLOGRAFT_REJECTION	0.3889	0.000	0.00539
HALLMARK_KRAS_SIGNALING_DN	0.3559	0.002	0.02094
HALLMARK_APICAL_JUNCTION	0.3409	0.003	0.02504
HALLMARK_ESTROGEN_RESPONSE_EARLY	0.3229	0.007	0.04455
HALLMARK_PANCREAS_BETA_CELLS	0.4555	0.080	0.05194
HALLMARK_APICAL_SURFACE	0.4070	0.097	0.06774
HALLMARK_GLYCOLYSIS	0.2935	0.056	0.12140
HALLMARK_APOPTOSIS	0.2945	0.057	0.12638
HALLMARK_BILE_ACID_METABOLISM	0.3017	0.149	0.20399

Note: Gene sets that were significantly enriched in CHOL1-pLKO-scramble-shRNA compared with CHOL1-pLKO-shFAXC#1.

Abbreviation: FDR, false discovery rate.

FAXC-knockdown cells (Table 2). Next, we determined whether FAXC is involved in the response to hypoxia and EMT. Hypoxia-inducible factor 1-α is an important factor in a hypoxic tumor microenvironment[35] and has been reported as a poor prognostic factor in CCA.[36] We measured the expression of HIF1-α in FAXC knockdown CHOL1 cells and found decreased HIF1-α expression in both in vitro cultured cells and xenografted tumor tissues (Figure 5E,F). We also assessed the phosphorylation of STAT3, which is a known modulator of EMT through EGF stimulation.[37,38] STAT3 Y705 and Y727 phosphorylation were suppressed in FAXC-knockdown CHOL1 cells (Figure 5G). CHOL1-pLKO-shFAXC#2 cells showed delayed STAT3 Y727 phosphorylation (Figure 5G).

4 | DISCUSSION

FAXC is a homolog of Fax in Drosophila, but the molecular characterization of Fax in Drosophila and FAXC in mammals has not been reported. Fax functions with Abl, a nonreceptor tyrosine kinase in Drosophila, in the development of an axon bundle in the central nervous system.[39] Fax knockdown results in a shortening of the protrusions of Drosophila escort cells, which are required for the maintenance of GSCs, and the loss of GSCs.[40] The present study is the first to report that FAXC is required for tumor development in human CCA and interacts with

ANXA2 and c-SRC. FAXC knockdown resulted in the suppression of CCA tumorigenesis and a reduction of HIF1-α expression, but did not affect proliferation, migration, or ALDH activity in monolayer cultures (Figure S6). This suggests that the FAXC gene may be required for in vivo proliferation, in which cancer cells intercommunicate with stromal cells and grow in the tumor microenvironment,[41] rather than simply affecting cell proliferation or migration.

ANXA2 is a tumor-promoting factor.[42] High ANXA2 expression occurs in several cancers, such as acute lymphoblastic leukemia, breast cancer, colorectal carcinoma, glioma, and hepatocellular carcinoma.[43] The biological function and localization of ANXA2 are regulated by its phosphorylation. Phosphorylation at S25 by protein kinase C is associated with secretion, whereas Y24 phosphorylation by c-SRC results in tumor progression, including tumorigenicity, EMT, invasion, and metastasis.[44,45] FAXC enhances the phosphorylation through c-SRC, suggesting that FAXC promotes CCA malignancy through ANXA2 phosphorylation.

Structurally, FAXC has a transmembrane domain and a binding domain for ANXA2 in its N- and C-terminal regions, respectively. FAXC also contains GST_N and GST_C domains, which were originally identified in MTX1.[46] Metaxin 1 localizes to the mitochondrial outer membrane to control mitochondrial permeability during the early phase of apoptosis. Additionally, MTX1 is phosphorylated by c-Abl, a nonreceptor tyrosine-protein kinase.[47] Metaxin 1 contains the

Gene set	Enrichment score	p value	FDR q value
KRAS.LUNG.UP.V1_UP	0.5804	0.000	0.000
KRAS.LUNG.BREAST_UP.V1_UP	0.5689	0.000	0.000
KRAS.600.LUNG.BREAST_UP.V1_UP	0.4876	0.000	0.000
KRAS.600_UP.V1_UP	0.4800	0.000	0.000
KRAS.300_UP.V1_UP	0.5186	0.000	0.000
KRAS.BREAST_UP.V1_UP	0.5137	0.000	0.000
KRAS.50_UP.V1_UP	0.6061	0.000	0.000
P53_DN.V2_UP	0.4905	0.000	0.000
EGFR_UP.V1_UP	0.4554	0.000	0.000
KRAS.KIDNEY_UP.V1_UP	0.4821	0.000	1.33E-04
MEL18_DN.V1_UP	0.4575	0.000	1.21E-04
STK33_NOMO_UP	0.4208	0.000	3.18E-04
BMI1_DN.V1_UP	0.4559	0.000	2.94E-04
P53_DN.V1_DN	0.4377	0.000	2.73E-04
RPS14_DN.V1_UP	0.4366	0.000	5.10E-04
SNF5_DN.V1_DN	0.4406	0.000	5.65E-04
SINGH_KRAS_DEPENDENCY_ SIGNATURE	0.6255	0.004	5.32E-04
LEF1_UP.V1_UP	0.4270	0.000	5.68E-04
CAHOY_ASTROGLIAL	0.4621	0.000	5.38E-04
KRAS.PROSTATE_UP.V1_UP	0.4529	0.000	6.37E-04

Note: Gene sets that were significantly enriched in CHOL1-pLKO-scramble-shRNA compared with CHOL1-pLKO-shFAXC#1.

Abbreviation: FDR, false discovery rate.
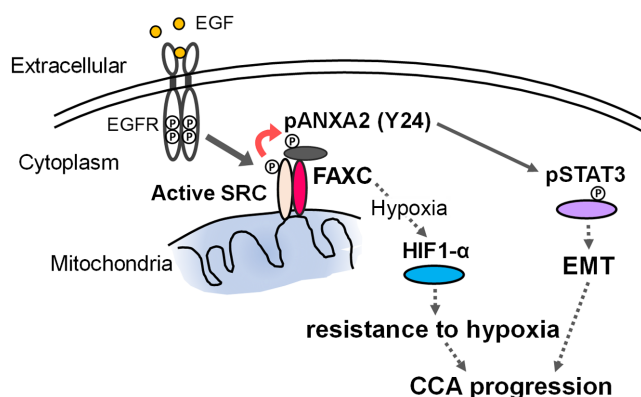
FIGURE 6 Model of the failed axon connection homolog (FAXC) pathway in cholangiocarcinoma (CCA). EGF, epidermal growth factor; EGFR, EGF receptor; EMT, epithelial–mesenchymal transition; HIF1-α, hypoxia-inducible factor 1-α.

TOM37 domain, also known as SAM37, which is a component of the mitochondrial outer membrane sorting assembly machinery (SAM or TOM) complex. Notably, human FAXC is found in the TOM37 domain.[46] These data are consistent with our findings that FAXC localizes to the mitochondria. In addition, ANXA2 is phosphorylated by c-SRC and receptor tyrosine kinases, such as the EGF receptor,[48] insulin receptor,[49] and platelet-derived growth factor,[50] at the plasma membrane. ANXA2 and c-SRC localize to the plasma membrane and

mitochondria.[51–53] In the present study, FAXC was localized to the mitochondria. Taken together, FAXC, ANXA2, and c-SRC complexes may form in the mitochondria and promote the phosphorylation of ANXA2, which promotes tumorigenesis.

Based on our RNA sequencing data, *FAXC*-knockdown CCA xenografts showed a negative correlation with the HYPOXIA and EMT gene sets. We also found that FAXC regulates HIF1-α expression levels. Previously, WDR5, which is a component of the histone methyltransferase complex, regulates HIF1-α expression levels by interacting with c-Myc in CCA.[54] FAXC regulates HIF1-α expression levels through an unidentified transcriptional mechanism; however, further studies are needed to define this process. In glioma or breast cancer cells, ANXA2 is required for adaptation to EMT and hypoxia.[38,55] Y24-phosphorylated ANXA2 binds STAT3, resulting in the promotion of EMT in breast cancer.[37] We determined that FAXC regulates the phosphorylation of ANXA2 and STAT3, which may promote EMT through the ANXA2/ STAT3 axis. Epithelial–mesenchymal transition induces cancer stem cell-like phenotypes, including tumorigenicity.[56,57] These results are consistent with our data. In addition, mitochondrial phospho-STAT3 (S727) promotes colony formation of RAS-transformed cancer cells,[58] which supports our model of a FAXC/ANXA2/c-Src complex in the mitochondria. Taken together, our data suggest that FAXC regulates the response to hypoxia through HIF1 and the promotion of EMT through the enhancement of Y24 phosphorylation of ANXA2 at mitochondria, which promotes CCA tumorigenesis (Figure 6).

KRAS-related signaling is suppressed by FAXC knockdown in xenograft CHOL1 cells. The interaction between KRAS and FAXC/ANXA2 has not been previously reported. Because KRAS signaling is enhanced in various cancers, including CCA,[59] and FAXC is a cancer-promoting factor in CCA, further studies are needed to elucidate the relationships between KRAS and FAXC.

In conclusion, we identified for the first time that FAXC is essential for CCA development and determined its localization, and characterized its interactions with other proteins (Figure 6). The findings of this study advance the current understanding of tumorigenesis mechanisms and identify potential therapeutic targets for CCA.

ORCID

Haruna Fujimori https://orcid.org/0009-0008-8855-1216
Michiaki Unno https://orcid.org/0000-0002-2145-6416
Keiichi Tamai https://orcid.org/0000-0003-0813-5885

REFERENCES

1. Saha SK, Zhu AX, Fuchs CS, Brooks GA. Forty-year trends in cholangiocarcinoma incidence in the U.S.: intrahepatic disease on the rise. *Oncologist*. 2016;21(5):594-599. doi:10.1634/theoncologist.2015-0446

2. Jarnagin WR, Fong Y, DeMatteo RP, et al. Staging, resectability, and outcome in 225 patients with hilar cholangiocarcinoma. *Ann Surg*. 2001;234(4):507-517. doi:10.1097/00000658-200,110,000-00010

3. Jusakul A, Cutcutache I, Yong CH, et al. Whole-genome and epigenomic landscapes of etiologically distinct subtypes of cholangiocarcinoma. *Cancer Discov*. 2017;7(10):1116-1135. doi:10.1158/2159-8290.CD-17-0368

4. Hanahan D. Hallmarks of cancer: new dimensions. *Cancer Discov*. 2022;12(1):31-46. doi:10.1158/2159-8290.CD-21-1059

5. Fujii E, Suzuki M, Matsubara K, et al. Establishment and characterization of in vivo human tumor models in the NOD/SCID/γcnull mouse. *Pathol Int*. 2008;58(9):559-567. doi:10.1111/j.1440-1827.2008.02271.x

6. Magee JA, Piskounova E, Morrison SJ. Cancer stem cells: impact, heterogeneity, and uncertainty. *Cancer Cell*. 2012;21(3):283-296. doi:10.1016/j.ccr.2012.03.003

7. Frame MC. Src in cancer: deregulation and consequences for cell behaviour. *Biochim Biophys Acta BBA—Rev Cancer*. 2002;1602(2):114-130. doi:10.1016/S0304-419X(02)00040-9

8. Erikson E, Erikson RL. Identification of a cellular protein substrate phosphorylated by the avian sarcoma virus-transforming gene product. *Cell*. 1980;21(3):829-836. doi:10.1016/0092-8674(80)90446-8

9. Radke K, Gilmore T, Martin GS. Transformation by Rous sarcoma virus: a cellular substrate for transformation-specific protein phosphorylation contains phosphotyrosine. *Cell*. 1980;21(3):821-828. doi:10.1016/0092-8674(80)90445-6

10. Roskoski R. Src kinase regulation by phosphorylation and dephosphorylation. *Biochem Biophys Res Commun*. 2005;331(1):1-14. doi:10.1016/j.bbrc.2005.03.012

11. Yuan J, Yang Y, Gao Z, et al. Tyr23 phosphorylation of Anxa2 enhances STAT3 activation and promotes proliferation and invasion of breast cancer cells. *Breast Cancer Res Treat*. 2017;164(2):327-340. doi:10.1007/s10549-017-4271-z

12. Wu B, Zhang F, Yu M, et al. Up-regulation of Anxa2 gene promotes proliferation and invasion of breast cancer MCF-7 cells. *Cell Prolif*. 2012;45(3):189-198.

13. Bharadwaj A, Bydoun M, Holloway R, Waisman D. Annexin A2 Heterotetramer: structure and function. *Int J Mol Sci*. 2013;14(3):6259-6305. doi:10.3390/ijms14036259

14. Fan Y, Si W, Ji W, et al. Rack1 mediates tyrosine phosphorylation of Anxa2 by Src and promotes invasion and metastasis in drug-resistant breast cancer cells. *Breast Cancer Res*. 2019;21:1-16.

15. Long Y, Chong T, Lyu X, et al. FOXD1-dependent RalA-ANXA2-Src complex promotes CTC formation in breast cancer. *J Exp Clin Cancer Res*. 2022;41(1):301. doi:10.1186/s13046-022-02504-0

16. Imai T, Tamai K, Oizumi S, et al. CD271 defines a stem cell-like population in hypopharyngeal cancer. *PLoS One*. 2013;8(4):e62002. doi:10.1371/journal.pone.0062002

17. Mochizuki M, Tamai K, Imai T, et al. CD271 regulates the proliferation and motility of hypopharyngeal cancer cells. *Sci Rep*. 2016;6:30707. doi:10.1038/srep30707

18. R Core Team. *R: A Language and environment for statistical computing*. R Foundation for Statistical Computing; 2023. https://www.R-project.org/

19. Nueda MJ, Tarazona S, Conesa A. Next maSigPro: updating maSigPro bioconductor package for RNA-seq time series. *Bioinforma Oxf Engl*. 2014;30(18):2598-2602. doi:10.1093/bioinformatics/btu333

20. Dobin A, Davis CA, Schlesinger F, et al. STAR: ultrafast universal RNA-seq aligner. *Bioinforma Oxf Engl*. 2013;29(1):15-21. doi:10.1093/bioinformatics/bts635

21. Kluin RJC, Kemper K, Kuilman T, et al. XenofilteR: computational deconvolution of mouse and human reads in tumor xenograft sequence data. *BMC Bioinformatics*. 2018;19(1):366. doi:10.1186/s12859-018-2353-5

22. Liao Y, Smyth GK, Shi W. featureCounts: an efficient general purpose program for assigning sequence reads to genomic features. *Bioinforma Oxf Engl*. 2014;30(7):923-930. doi:10.1093/bioinformatics/btt656

23. Love MI, Huber W, Anders S. Moderated estimation of fold change and dispersion for RNA-seq data with DESeq2. *Genome Biol*. 2014;15(12):550. doi:10.1186/s13059-014-0550-8

24. Subramanian A, Tamayo P, Mootha VK, et al. Gene set enrichment analysis: a knowledge-based approach for interpreting genome-wide expression profiles. *Proc Natl Acad Sci USA*. 2005;102(43):15545-15550. doi:10.1073/pnas.0506580102

25. Tamai K, Nakamura-Shima M, Shibuya-Takahashi R, et al. BEX2 suppresses mitochondrial activity and is required for dormant cancer stem cell maintenance in intrahepatic cholangiocarcinoma. *Sci Rep*. 2020;10(1):21592. doi:10.1038/s41598-020-78539-0

26. Hong Z, Jiang J, Lan L, et al. A polycomb group protein, PHF1, is involved in the response to DNA double-strand breaks in human cell. *Nucleic Acids Res*. 2008;36(9):2939-2947. doi:10.1093/nar/gkn146

27. Kamimura R, Uchida D, Kanno S, et al. Identification of binding proteins for TSC22D1 family proteins using mass spectrometry. *Int J Mol Sci*. 2021;22(20):10913. doi:10.3390/ijms222010913

28. Palmer I, Wingfield PT. Preparation and extraction of insoluble (inclusion-body) proteins from Escherichia coli. *Curr Protoc Protein Sci Editor Board John E Coligan Al*. 2012;6:6.3.1-6.3.20. doi:10.1002/0471140864.ps0603s70

29. Chakraborty A, Boel NME, Edkins AL. HSP90 interacts with the fibronectin N-terminal domains and increases matrix formation. *Cells*. 2020;9(2):272. doi:10.3390/cells9020272

30. Umekawa Y, Ito K. Thioredoxin o-mediated reduction of mitochondrial alternative oxidase in the thermogenic skunk cabbage Symplocarpus renifolius. *The Journal of Biochemistry*. 2019;165:57-65.

31. Tsumoto K, Umetsu M, Yamada H, Ito T, Misawa S, Kumagai I. Immobilized oxidoreductase as an additive for refolding inclusion bodies: application to antibody fragments. *Protein Eng Des Sel*. 2003;16(7):535-541. doi:10.1093/protein/gzg064

32. Cui HY, Wang SJ, Miao JY, et al. CD147 regulates cancer migration via direct interaction with annexin A2 and DOCK3-β-catenin-WAVE2 signaling. *Oncotarget*. 2016;7(5):5613-5629. doi:10.18632/oncotarget.6723

33. Kobayashi S, Yamada-Okabe H, Suzuki M, et al. LGR5-positive colon cancer stem cells interconvert with drug-resistant LGR5-negative cells and are capable of tumor reconstitution. *Stem Cells Dayt Ohio*. 2012;30(12):2631-2644. doi:10.1002/stem.1257

34. Cuenda A. Mitogen-activated protein kinases (MAPK) in cancer. In: Boffetta P, Hainaut P, eds. (Eds.)*Encyclopedia of Cancer*. 3rd ed. Academic Press; 2019:472-480. doi:10.1016/B978-0-12-801,238-3.64980-2

35. Jin X, Dai L, Ma Y, Wang J, Liu Z. Implications of HIF-1α in the tumorigenesis and progression of pancreatic cancer. *Cancer Cell Int*. 2020;20(1):273. doi:10.1186/s12935-020-01370-0

36. Morine Y, Shimada M, Utsunomiya T, et al. Hypoxia inducible factor expression in intrahepatic cholangiocarcinoma. *Hepato-Gastroenterology*. 2011;58(110–111):1439-1444. doi:10.5754/hge11156

37. Wang T, Yuan J, Zhang J, et al. Anxa2 binds to STAT3 and promotes epithelial to mesenchymal transition in breast cancer cells. *Oncotarget*. 2015;6(31):30975-30992. doi:10.18632/oncotarget.5199

38. Zhao S, Li B, Zhao R, et al. Hypoxia-induced circADAMTS6 in a TDP43-dependent manner accelerates glioblastoma progression via ANXA2/NF-κB pathway. *Oncogene*. 2023;42(2):138-153. doi:10.1038/s41388-022-02542-0

39. Hill KK, Bedian V, Juang JL, Hoffmann FM. Genetic interactions between the drosophila Abelson (Abl) tyrosine kinase and failed axon connections (fax), a novel protein in axon bundles. *Genetics*. 1995;141(2):595-606.

40. Su YH, Rastegri E, Kao SH, et al. Diet regulates membrane extension and survival of niche escort cells for germline homeostasis via insulin signaling. *Development*. 2018;145(7):dev159186.

41. Li Y, Zhao L, Li XF. Hypoxia and the tumor microenvironment. *Technol Cancer Res Treat*. 2021;20:15330338211036304. doi:10.1177/15330338211036304

42. Wang T, Wang Z, Niu R, Wang L. Crucial role of Anxa2 in cancer progression: highlights on its novel regulatory mechanism. *Cancer Biol Med*. 2019;16(4):671-687. doi:10.20892/j.issn.2095-3941.2019.0228

43. Wang CY, Lin CF. Annexin A2: its molecular regulation and cellular expression in cancer development. *Dis Markers*. 2014;2014:1-10.

44. Grindheim AK, Saraste J, Vedeler A. Protein Phosphorylation and its Role in the Regulation of Annexin A2 Function. *Biochim Biophys Acta BBA−Gen Subj*. 2017;1861(11 Part A):2515-2529. doi:10.1016/j.bbagen.2017.08.024

45. Zhang HJ, Yao DF, Yao M, et al. Annexin A2 silencing inhibits invasion, migration, and tumorigenic potential of hepatoma cells. *World J Gastroenterol*. 2013;19(24):3792-3801. doi:10.3748/wjg.v19.i24.3792

46. Adolph KW. FAXC proteins of vertebrates and invertebrates: relationship to metaxin proteins. 2023. doi:10.1101/2023.01.04.522723

47. Petit E, Cartron PF, Oliver L, Vallette FM. The phosphorylation of Metaxin 1 controls Bak activation during TNFα induced cell death. *Cell Signal*. 2017;30:171-178. doi:10.1016/j.cellsig.2016.11.008

48. Dziduszko A, Ozbun MA. Annexin A2 and S100A10 regulate human papillomavirus type 16 entry and intracellular trafficking in human keratinocytes. *J Virol*. 2013;87(13):7502-7515. doi:10.1128/JVI.00519-13

49. Rescher U, Ludwig C, Konietzko V, Kharitonenkov A, Gerke V. Tyrosine phosphorylation of annexin A2 regulates rho-mediated Actin rearrangement and cell adhesion. *J Cell Sci*. 2008;121(13):2177-2185. doi:10.1242/jcs.028415

50. Brambilla R, Zippel R, Sturani E, Morello L, Peres A, Alberghina L. Characterization of the tyrosine phosphorylation of calpactin I (annexin II) induced by platelet-derived growth factor. *Biochem J*. 1991;278(2):447-452. doi:10.1042/bj2780447

51. Koc EC, Hunter CA, Koc H. Phosphorylation of mammalian mitochondrial EF-Tu by Fyn and c-Src kinases. *Cell Signal*. 2023;101:110524. doi:10.1016/j.cellsig.2022.110524

52. Aukrust I, Rosenberg LA, Ankerud MM, et al. Post-translational modifications of annexin A2 are linked to its association with perinuclear nonpolysomal mRNP complexes. *FEBS Open Bio*. 2017;7(2):160-173. doi:10.1002/2211-5463.12173

53. Liu Y, Zhu J, Liu J, et al. Over-expression of gastrin inhibits apoptosis of gastric cancer cells via reactive oxygen species and annexin A2-mediated mitochondrial dysfunction. *Int J Morphol*. 2023;41(1):308-318. doi:10.4067/S0717-95022023000100308

54. Chen T, Li K, Liu Z, et al. WDR5 facilitates EMT and metastasis of CCA by increasing HIF-1α accumulation in Myc-dependent and independent pathways. *Mol Ther*. 2021;29(6):2134-2150. doi:10.1016/j.ymthe.2021.02.017

55. Chen CY, Lin YS, Chen CH, Chen YJ. Annexin A2-mediated cancer progression and therapeutic resistance in nasopharyngeal carcinoma. *J Biomed Sci*. 2018;25(1):30. doi:10.1186/s12929-018-0430-8

56. Zhang L, Chen W, Liu S, Chen C. Targeting breast cancer stem cells. *Int J Biol Sci*. 2023;19(2):552-570. doi:10.7150/ijbs.76187

57. Wellner U, Schubert J, Burk UC, et al. The EMT-activator ZEB1 promotes tumorigenicity by repressing stemness-inhibiting microRNAs. *Nat Cell Biol*. 2009;11(12):1487-1495. doi:10.1038/ncb1998

58. Gough DJ, Corlett A, Schlessinger K, Wegrzyn J, Larner AC, Levy DE. Mitochondrial STAT3 supports Ras-dependent oncogenic transformation. *Science*. 2009;324(5935):1713-1716. doi:10.1126/science.1171721

59. Uprety D, Adjei AA. KRAS: from undruggable to a druggable cancer target. *Cancer Treat Rev*. 2020;89:102070. doi:10.1016/j.ctrv.2020.102070

SUPPORTING INFORMATION

Additional supporting information can be found online in the Supporting Information section at the end of this article.